International Journal of Control and Automation
Vol.7, No.2 (2014), pp.297-308
http://dx.doi.org/10.14257/ijca.2014.7.2.27

Test and Analysis of Micro-vibrations Generated by Large Control Moment Gyroscope

Xue Li [1] and Wei Cheng [2]

[1] *School of Aeronautical Science and Engineering, Beihang University, NO.37, Xueyuan Road, Beijing 100191, China*
[2] *School of Aeronautical Science and Engineering, Beihang University, NO.37, Xueyuan Road, Beijing 100191, China*

1daxue129.student@sina.com, 2cheng_wei@buaa.edu.cn

Abstract

Control moment gyroscope (CMG) is widely used as an actuator of spacecraft attitude control Micro-vibrations generated by CMG will influence the performance of high-sensitivity instruments on-board the spacecraft; however, the micro-vibrations characteristics of CMG are not yet clearly understood. This paper concentrates on testing and analyzing the micro-vibrations produced by CMG. Firstly, for the massive weight of CMG, it is impossible to remove the influence of testboard's inherent characteristic on CMG's vibration disturbance cannot be isolated with improving testboard stiffness. Hence, a rigid CMG model was developed and used in the control experiment for comparing the modal test results of the CMG model and prototype. Secondly, considering the natural frequency of CMG should be different according to the vitiation of its rigidity and mass distribution, a CMG start up dynamic test was implemented to calculate the working CMG natural frequency. Finally, a dis turbing frequency test under multiple CMG gimbal angular speed was designed to calculate t he influence from the CMG gimbal angular and its rotation speed and to further provide data for whole satellite CMG vibration disturbance analysis.

Key words: *CMG; micro- disturbance; disturbance characteristics test; result analysis*

1. Introduction

The micro-vibrations produced by mechanical systems onboard spacecraft, for example, reaction/momentum wheel assemblies (R/MWA), Control Moment Gyroscope (CMG), cryo-coolers and solar panel deployment actuator, can degrade the performance of instruments with high pointing precision and stability. Of these, momentum exchange actuators for spacecraft altitude control, such as R/MWAs and CMG, are the most prominent sources of disturbance [1, 2].

Although R/MWAs and CMG both achieve reaction torque via high speed rotary flywheels, their operating principles are different [16]. R/MWAs provide control torque for spacecraft by adjusting the rotational acceleration of the flywheel, which operates at nominal zero (RWA) or non-zero (MWA) bias velocity [3, 4]. CMG generate gyroscopic torques by gimballing the angular momentum vector of the flywheel, which is gimballed and usually operates with a constant rotating speed that is much larger than the maximum of the R/MWA (as high as 6000–10,000 rev/min) [2].

Control moment gyroscope (CMG) achieves spacecraft attitude change through the angular momentum change of the flywheel which is forced by frame rotation. Disturbance generated

ISSN: 2005-4297 IJCA

by the flywheel results primarily from the following: flywheel mass imbalance, internal resonance, imperfection in mechanical bearings and motor ripple. There has been a significant amount of research addressing the micro-vibration of rotary flywheels.

Most papers published focus on disturbance produced by flywheel mass imbalance and consider it as the largest disturbance source [4-8, 14-15, 17] or analyze the disturbance sources separately. The amplitudes of disturbance forces and torques, originate from the imbalance of mass distribution, are highly coherent to the square of the angular velocity. Meanwhile, due to fundamental harmonic, the frequency of disturbance is equal to the rotation frequency. Internal resonance would take place while the disturbance harmonics crossed the flywheel structural modes. This phenomenon was raised by Masterson *et al.* [7], and a linear flywheel dynamic model, with five degrees of freedom for the RWA, was created to capture the interaction between the structural modes and fundamental harmonic. Additional stimulant, brought from the bearings which support the flywheel, was introduced due to imperfections of the retainer. A sub-harmonic, with an approximately 0.6 times fundamental harmonic frequency, was found by Shigemune and Yoshiaki [6] for the imperfections of the nonholonomically constrained bearing retainer. The rotation elements and raceways of the bearings provide compliant mechanism support, which allows the flywheel to translate rock and amplify the disturbance force and torque. Furthermore, in high rotation speed, non-linear elastic contact and clearance in the bearing assemblies would always result in nonlinearities.

A number of methods have been evaluated to measure flywheel induced micro-vibrations. For example, Elis and Miller [12] have proposed a coupled disturbance analysis method using dynamic mass measurement techniques. Shigemune and Yoshiaki [6] designed a new air-float disturbance detector based on a CCD laser displacement transducer with a resolution of 0.01 μm; this method is effective in measuring the lower frequency disturbance generated by WAs. Zhou *et al.* [14] have developed a Seismic Micro-Vibration Measurement System (SMVMS) to test the micro-vibration produced by a cantilevered MWA: a method that is cost effective and provides excellent noise immunity. Generally, the methods mentioned above can indirectly acquire disturbance forces/torques by detecting the disturbance displacements or accelerations. Masterson *et al.* [8] established a system of disturbance measurements by using the Kistler table: a dynamometer platform with measurement precision greater than 0.01 N that can directly detect disturbance forces/torques [16].

The majority of domestic researches focused on the dynamics modeling and simulation of disturbance model of large control moment gyroscope, yet the experimental research field remains untouched. In this paper describes the vibration disturbance test of one large control moment gyroscope.

Since the biggest feature of this CMG is its large mass moving parts, the most direct outcome will be an obvious reduced-fundamental frequency of the system when the CMG is installed on the testboard. Therefore, the influence of testboard's inherent characteristic on CMG's vibration disturbance cannot be isolated with improving testboard stiffness. In order to analyze and isolate the influence of testboard dynamic characteristic on experiment outcome, two forms of brackets, namely A and B, are designed as followed: Bracket A has a four-arc-pillar as its upper structure; Bracket B has an upper structure same as the original CMG's vibration test bracket. At the same time, the comparison test results of CMG's stiffness simulated model and original part, CMG startup dynamic test, along with dynamic tests under different gimbal angular velocities are designed to test and analyze CMG's vibration disturbance characteristics.

2. Mathematical Model

According to the model from the Masterson from MIT [7], we know the mathematical model of the CMG, when the low speed shaft is locked, that is:

$$m(t)=\sum_{i=1}^{n} C_i \sin(h_i \Omega t) \quad . \tag{1}$$

$$f_i = h_i \Omega \tag{2}$$

Where, $m(t)$ is the disturbance force or torque in Newton's (N) or Newton-meters ($N \cdot m$), n is the number of harmonics included in the model, Ω is the rotating speed of CMG, h_i is the i^{th} harmonic number, f_i is the frequency multiplication of harmonic, C_i is the amplitude of frequency multiplication of harmonic, the units is still N / Hz^2 or $N \cdot m / Hz^2$. In this paper, CMG's rotation rate is 9500rpm, so its fundamental frequency is:

$$f = \frac{9500}{60} \approx 158.3 Hz \tag{3}$$

In order to improve the above model only considering the active force, This paper propose the improved version of the model [9], but this part isn't the main part:

$$m(t) = \sum_{i=1}^{n} \tilde{C}_i \beta_i(h_i \Omega) \Omega^2 \sin(2\pi h_i \Omega t + \alpha_i) \tag{4}$$

Where, $\tilde{C}_i$ is the improved amplitude of frequency multiplication of harmonic, the units is still N / Hz^2 or $N \cdot m / Hz^2$, $\beta_i(h_i \Omega)$ [4] is the amplification coefficient caused by the Inherent characteristics of CMG's internal structure.

During bearing is in the rotation, Rotation of the body scrolls between the inner and outer ring [10], if the rolling surface defects due to the manufacturing precision or breakage, rolling bodies will generate an alternating excited force. This force depends on many factors, including the defect, the bearing, the diameter and number of bearing balls, it's mainly performance for in the form of multiple harmonics of flywheel speed. That is:

$$m(t) \propto \Omega^2 \sin(2\pi h_i \Omega t) \qquad i = 1,2, \cdots, n \quad . \tag{5}$$

Where, hi is the order of harmonics (Can be a decimal), n is the sum of all the order harmonics.

The bearing's form used in this paper is the inner ring fixed, the outer ring rotating with the shaft, considering the case of the axial force, the main harmonic coefficients are:

Rotate with the shaft：

$$h_i = \frac{1}{2}\left(1 + \frac{d}{D_m}\cos\alpha\right) = 0.4 \tag{6}$$

Defect of outer ring：

$$h_i = \frac{1}{2}\left(1 - \frac{d}{D_m}\cos\alpha\right) Z = 5.5. \tag{7}$$

Where, Z is the sum of rolling elements, D_i is the diameter of inner ring raceway, D_0 is the diameter of outer ring raceway, D_m is the diameter of raceway, The coefficient determines the test result will exist non-integer harmonic frequencies like 0.4 and 5.5 octave, *etc.*

3. Test of CMG's Inherent Characteristics

The natural frequency of rotating machinery can be measured in two ways: free vibration method and stimulating vibration load method. During the test, free vibration method used hammering method while stimulating vibration load method applied an un-increased rotation speed method in CMG's startup period to realize frequency scan. The test speed was from 0rmp to 9500rmp. When CMG's rotor gradually increased its speed, changes took place in CMG's natural frequency (including "V" Line) as well as its mounting structural frequency. Based on the comparison of these two methods, a clearer picture of CMG's natural frequency under working mode can be obtained.

3.1 Comparison Test of CMG's Simulated Model and Original Objects

Since the inherent characteristic of the testboard cannot be isolated from that of the CMG under low coupling, the frequency measured during the modeling test after the large CMG being installed on the testboard can be categorized into two kinds: CMG inherent frequency featured as its structure; and mounting structural frequency featured as mounting structure.

A simulated model which has the same (with an error less than 3%) mass, gravitational center and moment of inertia with the original CMG object was constructed and installed on the testboard in the same way as the original one so as to carry out a modeling comparison test, as shown in Figure 1. Compared to the testboard, the simulated model can be regarded as a rigid object. After its installation on the testboard, the top five modal bands of the test result include two direction bendings, one contortion, and two translational modals. However, the results of the test on the original CMG object are more significant than that on the model, and the discrepancy is considered the natural frequency of CMG. In this way, it enables the calculation of the natural and mounting frequencies of a stationary CMG.

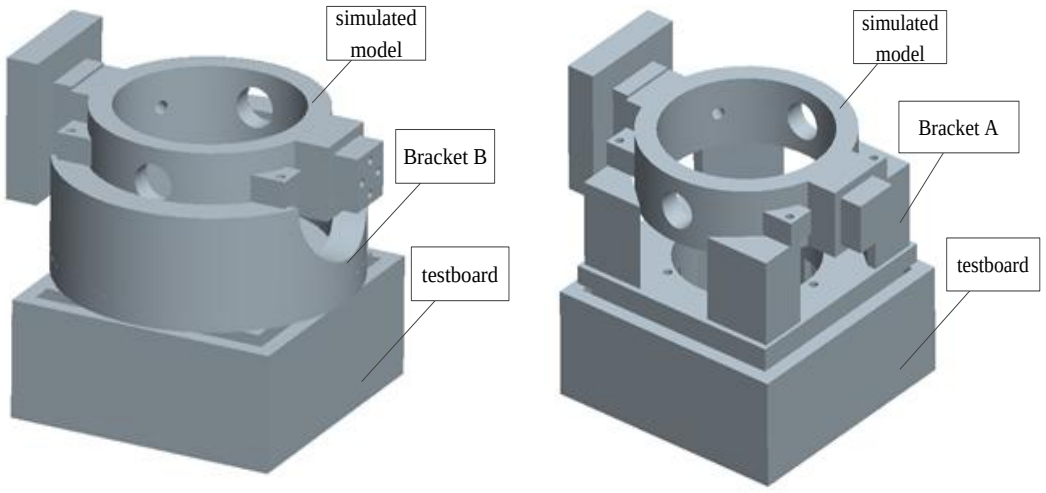

（a） （b）

Figure 1. 3D Experimental system: (a) refers to Bracket A form, (b) refers to Bracket B form

To compare models, the simulated model and original objects are installed on the testboard in the same manner. Hammering method was used in the test and was implemented in a multi-point hammering and one position acceleration measurement way. Also, according to the transfer function among one point and another, major natural frequency and modals can be measured. The sampling frequency is set to 2048 Hz, and the interval is 16s. Considering a complex coupling characteristic of CMG and other installation systems when frequency exceeds 500Hz, quantification measurement was utilized for amplitude as well as frequency between 0 and 500Hz. Yet, for frequency between 500Hz and 1000Hz, only some necessary vibration disturbance frequency monitoring was needed so as to obtain quantitative data which had no further data precision requirement, thus to compare and infer vibration disturbance tendency and properties. Compared with the 500Hz frequency of the previous test, frequency distribution is as followed in Table 1.

Table 1. Frequency Features of Modal Test Between 0 and 500Hz[Hz] (Frequency of the mounting structure-FMS, CMG natural frequency-CNF)

Testboard + simulator （**Bracket A**）	Testboard + CMG （**Bracket A**）	Testboard + simulator （**Bracket B**）	Testboard + CMG （**Bracket B**）	Frequency Type
118	109	105	101	FMS
128	117	128	120	FMS
241	234	232	249	FMS
260	243			FMS
	310		317	CNF
	345		335	CNF
393	393	387	412	FMS
	456		445	CNF
	469		474	CNF

3.2 CMG Startup Test

In the startup test, the axis of the CMG structure is locked, and the rotation speed is increased from 0 rpm and then maintained at 9550 rpm. Overlaying the vibration disturbance signals' change in the startup test with the rotations speed's change and creates a waterfall figure which demonstrates the relationship between frequencies' change and rotation speed. Figure 2 is CMG startup test vibration disturbance Fx waterfall figure.

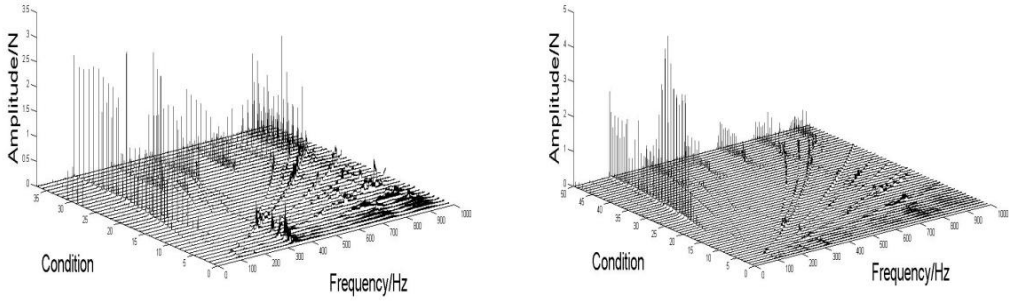

（a） （b）

Figure 2. CMG Startup Test Vibration Disturbance Fx Waterfall Figure (a) refers to Bracket A form, (b) refers to Bracket B form

Several kinds of frequencies can be identified from the waterfall figure of the startup test: frequency that would change with the change of rotation speed ("V" Line), harmonic wave (regression to the rotation speed), frequency that would not change with rotation speed. All the frequency distributions are shown in Table 2.

Table 2. Frequency Features Of Startup Test Between 0 and 1000Hz [Hz] (Octave Frequency- OF, Fundamental Frequency-FF)

Frequency Unrelated To Rotation Speed （ Bracket A）	Frequency Unrelated To Rotation Speed （ Bracket B）	Vibration Force Harmonic Frequency (9500 rpm) （ Bracket A）	Vibration Force Harmonic Frequency (9500 rpm) （ Bracket B）	V Line Frequency （ Bracket A）	V Line Frequency （ Bracket B）
109	105	65.75 (0.4 OF)	65.8（(0.4 OF）	174(0 rpm)to 153(9500 rpm)	179(0 rpm)to 151(9500 rpm)
117	121	158.3(FF)	158（Base Band）	174(0 rpm)to 312Hz(9500 rpm)	178(0 rpm)to 316Hz(9500 rpm)
233	235	316.7 (2 OF)	316（2 OF）		

244	312	394 (2.5 OF)	394(2.5 OF)		
309	335	475 (3 OF)	475（3 OF）		
345	364	633.3 (4 OF)	633（4 OF）		
370	412	791.5 (5 OF)	791（5 OF）		
394	445	872 (5.2 OF)	872（5.2 OF）		
456	467	921 (5.5 MF)	921（5.5 OF）		
469	612				
610	770				
762	806				
806	935				
933					

By comparison with the model simulation, 0.4 octave frequency, 2 octave frequency, 3 octave frequency, 5 octave frequency and 5.5 octave frequency are very obvious, but we can also find in the test 2.5 octave frequency and 5.8 octave frequency, the specific reason speculated that its internal low-speed bearings caused.

Based on the hammering and stimulating vibration load method, CMG's inherent structural frequency during the working condition can be measured. See Table 3-4 as followed.

Table 3. The various frequency of CMG's disturbance with bracket A [Hz] (Octave Frequency- OF, Fundamental Frequency-FF)

Frequency of the mounting structure	Vibration Force Harmonic Frequency (9500 rpm)	CMG Natural Frequency	
		Frequency Unrelated to Rotation	V Line Frequency
109	65.75 (0.4 OF)	309	174(0 rpm)to 153(9500 rpm)
117	158.3(FF)	345	174(0 rpm)to 312Hz(9500 rpm)
233	316.7（2 OF）	370	
243	394(2.5 OF)	456	
312	475（3 OF）	469	
394	633.3（4 OF）		
610	791.5（5 OF）		
762	872（5.2 OF）		
806	921（5.5 OF）		
933			

Table 4. The various frequency of CMG's disturbance with bracket B [Hz] (Octave Frequency- OF, Fundamental Frequency-FF)

Frequency of the mounting structure	Vibration Force Harmonic Frequency (9500 rpm)	CMG Natural Frequency	
		Frequency Unrelated to Rotation	V Line Frequency
105	65.8（0.4OF）	312	179(0 rpm)to 151(9500 rpm)
121	158（FF）	335	178(0 rpm)to 316Hz(9500 rpm)
235	316（2 OF）	364	
249	394(2.5 OF)	445	
412	475（3 OF）	467	
612	633（4 OF）		
770	791（5 OF）		
806	872（5.2 OF）		
935	921（5.5 OF）		

The discrepancy between stimulating vibration load method and hammering is considered to be the natural frequency of CMG (370Hz under Bracket A form; 364Hz under Bracket B form).

Due to the stiffness difference in these two brackets, there are certain differences in CMG's inherent frequency as well as "V" Line frequency measured under two kinds of installation conditions. Different installation conditions bring influences to CMG's inherent frequency, yet it remains to be rather small.

4. CMG's Vibration Disturbance Test

Except for the inherent frequency of CMG and its installation that exerts influence on CMG's vibration disturbance characteristic, rotation speed parameter (gimbal angle and rotation speed) is another factor. In order to measure the influence of this two factors, two kinds of tests were designed, respectively, steady-state test and dynamic-state test. The former one was used to identify gimbal angle's influence on CMG's vibration disturbance characteristic, while the latter one was used to measure both gimbal angle and rotation speed's influence on CMG's vibration disturbance characteristic.

4.1 Steady-state Test of CMG's Vibration Disturbance Characteristics

During the steady-state test, the axis of the CMG structure was locked, the rated speed of the rotor was 9500rpm, every 10°of gimbal angle from 0°to 350° was a measuring point, and altogether 36 operation modes were measured. Overlaying the vibration disturbance signals' change with gimbal angle's change and creates a waterfall figure. Figure 3 is steady-state test vibration disturbance Fx waterfall figure.

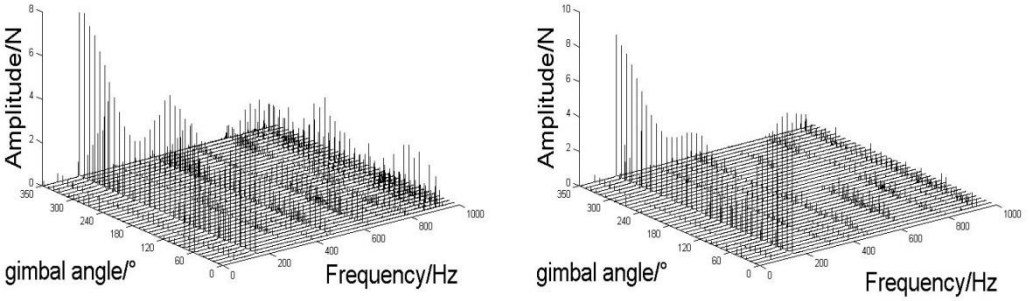

（a） （b）

Figure 3. Steady-state Test Vibration Disturbance Fx Waterfall Figure (a) refers to Bracket A form, (b) refers to Bracket B form

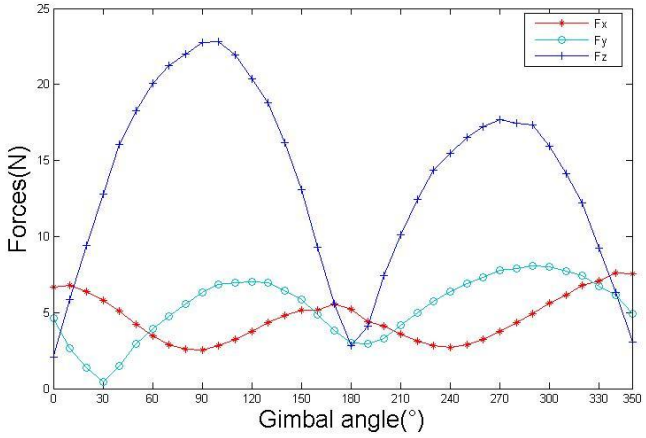

（a）

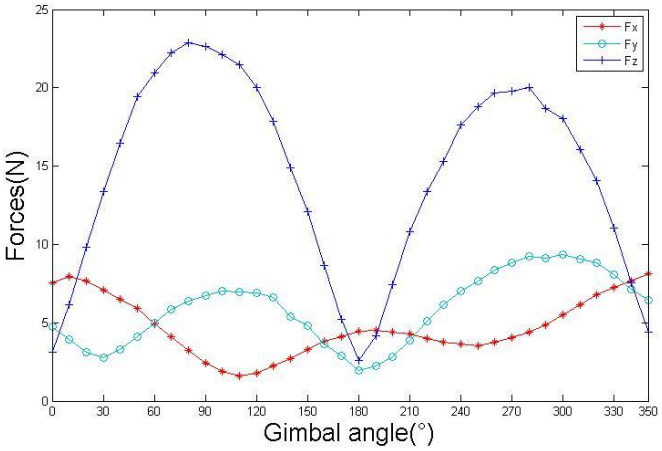

（b）

Figure 4. Disturbance force outputs under different gimbal angles at 158.3Hz (a) refers to Bracket A form, (b) refers to Bracket B form

4.2 Dynamic-state Test of CMG's Vibration Disturbance Characteristics

In respect to the features of CMG gimbal axis rotation speed, the dynamic-state test can be divided into low-speed rotation and high-speed rotation. In the low-speed rotation test, rotation speed under 1°/s was the focus. Overlaying the vibration disturbance signals' change with gimbal angle's change and creates a waterfall figure. And Figure 5 shows the situation of 0.1°/s rotation speed. High-speed rotation focused on rotation speed from 1°/s to 60°/s. Overlaying the vibration disturbance signals' change with gimbal angle's change and creates a waterfall figure, Figure 6.

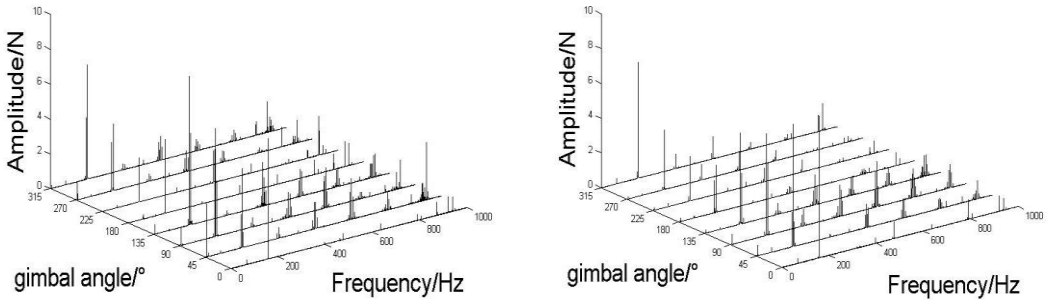

（a） （b）

Figure 5. Waterfall Figure of the Vibration Disturbance at 0.1°/s Rotation Speed: (a) refers to Bracket A form, (b) refers to Bracket B form

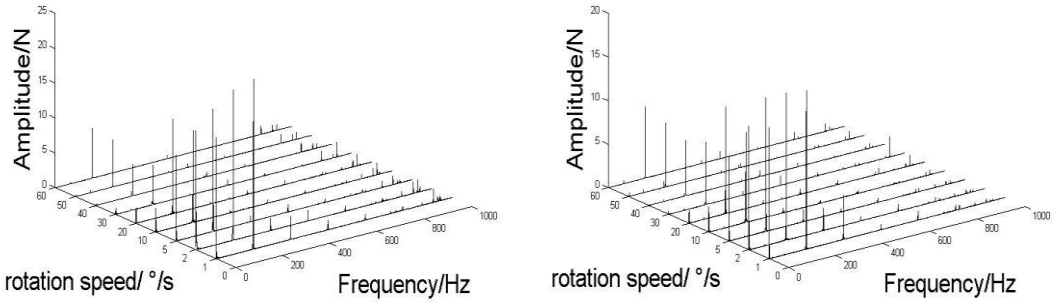

（a） （b）

Figure 6. Waterfall Figure of the Vibration Disturbance at High Rotation Speed: (a) refers to Bracket A form, (b) refers to Bracket B form

4.3 Test Result Analysis

1) Vibration disturbance frequency is represented by 158.3Hz base band and its frequency multiplication in the steady-state test while the 158.3 Hz base band has the most significant amplitude. When the harmonic wave's frequency multiplication is getting closer to CMG's inherent frequency or mounting frequency, satellite peak will appear in the harmonic wave of vibration force and its amplitude will increase.

2) The base band as well as other frequencies vary with the change of gimbal angle in the steady-state test. And there appears two wave crests with 180° in between.

3) In the steady-state test and low-speed rotation test, the amplitude of vibration disturbance mainly varies with the change of gimbal angle and the rotation speed of gimbal axis has no obvious influence on it. However, in high-speed rotation test, both the rotation speed of gimbal axis and gimbal angle's change have influences on the amplitude of vibration disturbance.

5. Conclusion

Based on the comparison test of CMG simulated model and its original objects installed under two different stiffness conditions, CMG startup test, as well as dynamic tests at different rotation speeds, this paper successfully obtained basic data of CMG's inherent characteristics and its vibration disturbance characteristics. What's more, this paper also provided a solid data support for the upcoming analysis on the whole satellite CMG vibration disturbance characteristic.

References

[1] L. Vaillon and C. Philippe, "Passive and active microvibration control for very high pointing accuracy space systems", Smart Materials and Structure, vol. 8, (**1999**), pp. 719-728.
[2] C. E. Eyerman, "A System Engineering Approach to Disturbance Minimization for Spacecraft Utilizing Controlled Structures Technology", Master Degree Thesis, Aeronautics and Astronautics, MIT, (**1990)**.
[3] T. Shigemune, K. Masahito, S. Makoto and O. Yoshiaki, "Analysis of retainer induced disturbances of reaction wheel", Journal of System Design and Dynamics, (**2007**), pp. 307–317, http://dx.doi.org/10.1299/jsdd.1.307.
[4] W. Y. Zhou, D. X. Li, Q. Luo and K. Liu, "Analysis and testing of microvibrations produced by momentum wheel assemblies", Chinese Journal of Astronautics, vol. 25, (**2012**), pp. 640–649, http://dx.doi.org/10.1016/s1000-9361, (11) 60430-5.
[5] L. P. Davis, J. F. Wilson, R. E. Jewell and J. J. Roden, "Hubble Space Telescope Reaction Wheel Assembly Vibration Isolation System", NASA Marshall Space Flight Centre, **(1986)**.
[6] T. Shigemune and O. Yoshiaki, "Experimental and numerical analysis of reaction wheel disturbances", JSME International Journal, Series C, vol. 46, (**2003**), pp. 519–526.
[7] R. A. Masterson, D. W. Miller and R. L. Grogan, "Development and validation of empirical and analytical reaction wheel disturbance models", Proceedings of the 1999 AIAA/ASME/ASCE/AHS/ASC Structures, Structural Dynamics and Materials Conference, St. Louis MO, (**1999)**.
[8] R. A. Masterson, D. W. Miller and R. L. Grogan, "Development and validation of reaction wheel disturbance models: empirical model", Journal of Sound and Vibration, vol. 249, (**2002**), pp. 575–598, http://dx.doi.org/10.1006/jsvi.2001.3868.
[9] P. F. Zhang, W. Cheng and Y. Zhao, "Disturbance Modeling and Parameters Identification of Reaction Wheel Assembly on Spacecraft", Journal of Beijing University of Aeronautics and Astronautics, vol. 36, no. 7, (**2010)**.
[10] S. W. Pang, L. Yang and G. J. Xu, "New Development of Micro-vibration Integrated Modeling and Assessment Technology for High Performance Spacecraft", Structure & Environment Engineering, vol. 37, no. 6, (**2007**).
[11] B. Q. Chang and X. Y. Qing, "Dynamic model of ball bearings with internal clearance and waviness", Journal of Sound and Vibration, vol. 294, (**2006**), pp. 23–48, http://dx.doi.org/10.1016/j.jsv.**2005**.10.005.
[12] L. M. Elias and D. W. Miller, "A coupled disturbances analysis method using dynamic mass measurement techniques", Proceedings of AIAA/ASME/ASCE/AHS/ASC Structures, Structural Dynamics, and Materials Conference, AIAA 2002-1252, **(2002)** April 22–25.
[13] T. Shigemune, K. Masahito, S. Makoto and O. Yoshiaki, "Analysis of retainer induced disturbances of reaction wheel", Transactions of the Japanese Society of Mechanical Engineering, vol. 71, no. 1, (**2005**), pp. 21–28.
[14] W. Y. Zhou, G. S. Aglietti and Z. Zhang, "Modeling and testing of a soft suspension design for a reaction/momentum wheel assembly", Journal of Sound and Vibration, vol. 330, (**2011**), pp. 4596–4610, http://dx.doi.org/10.1016/j.jsv.2011.03.028.

[15] W. Y. Zhou and D. X. Li, "Design and analysis of an intelligent vibration isolation platform for reaction/momentum wheel assemblies", Journal of Sound and Vibration, vol. 331, no. 13, (**2012**), pp. 2984-3005.
[16] Q. Luo, D. X. Li and W. Y. Zhou, "Dynamic modelling and observation of micro-vibrations generated by a Single Gimbal Control Moment Gyro", Journal of Sound and Vibration, vol. 332, no. 19, (**2013**), pp. 4403-4424.
[17] R. Van Riper, "Future technology trends for control moment gyroscopes", Proceedings of AIAA Guidance, Navigation and Control Conference, Williamsburg, VA, (**1986)** April.

Authors

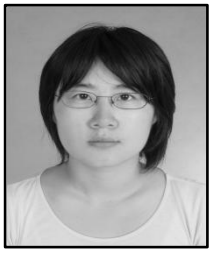

Xue Li. She is a Ph.D. candidate in Beihang University, Beijing, 100191, China. Her main research interest is micro-vibration analysis and control on spacecraft now.

Wei Cheng. He is a professor and a Ph.D. supervisor in Beihang University, Beijing, 100191, China. His main research interests are structural dynamics and vibration control.

